

## Application Note #139

# AFM and Raman Spectroscopy — Correlated Imaging and Tip Enhanced Raman Scattering

The desire to identify materials and their properties to understand complex systems and better engineer their functions has been driving scanning probe microscopies since their inception (see figure 1). Both atomic force microscopy (AFM) and Raman spectroscopy are techniques used to gather information about the surface properties and chemical information of a sample. There are many reasons to combine these two technologies, and this application note discusses both the complementary information gained from the techniques and how a researcher having access to a combined system can benefit from the additional information available.

### Two Surface Analysis Methods

**Atomic force microscopy** — In atomic force microscopy, a sharp tip is brought into close proximity with a sample and held at that distance by means of a force-based feedback loop.<sup>1</sup> In addition to the force on which the primary feedback loop is based, different quantities such as electrical current, surface potential, or specific nanomechanical properties can be measured. By scanning tip and sample relative to each other and measuring these quantities at discrete locations in a serial fashion, three-dimensional images of selected sample properties can be created. The information from atomic force microscopy has proven to be extremely useful for scientific research, but it lacks the chemical specificity available from vibrational spectroscopies.

**Raman spectroscopy** — Spectroscopy is the study of the interaction of electromagnetic radiation with matter. The most common kinds are X-ray, fluorescence, infrared, and Raman.<sup>2</sup> The latter two are vibrational techniques, i.e., the energy of radiation employed is sufficient to excite molecular or lattice vibrations. In a Raman experiment the sample is illuminated with monochromatic light, and the inelastically scattered light is detected. If a sample is illuminated with light of a frequency  $\nu_0$ , most of the scattered light is Rayleigh scattered, i.e., elastically scattered without a change in frequency. A small portion, however, is scattered at a different frequency  $\nu_1$  because of a change

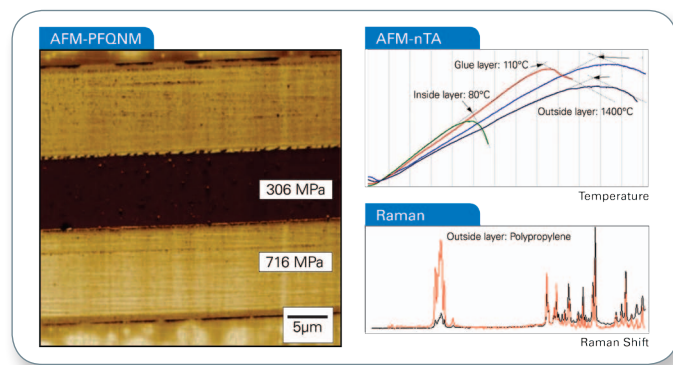


Figure 1. Atomic force microscopy and correlated optical spectroscopies can yield information about the sample composition (here a cross section of some food packaging material), shape, and various other properties, such as nanomechanical maps and thermal property maps.

in the polarizability of the illuminated molecule. This shift is referred to as the Stokes shift if  $\nu_1$  is red-shifted with regard to the incident light, or anti-Stokes if  $\nu_1$  is blue-shifted. A plot of the measured intensity of these shifts versus the frequency is referred to as a Raman spectrum and is a representation of the vibrational modes of the molecules or solids to be investigated or identified.

Raman spectroscopy can provide information about a variety of materials-related phenomena: (a) molecular composition by analyzing bands at characteristic frequencies (fingerprint); (b) symmetry or orientation of molecules or crystals by monitoring peaks using polarization selection for the incident and scattered light;<sup>4</sup> or (c) measurement of stress or strain in a crystal by analyzing e.g., the frequency shift of a characteristic Raman band. (See reference 5 for an in-depth review article on how Raman spectroscopy can be applied to popular carbon allotropes.)

As a direct probe of the vibrational structure, Raman does not depend on the presence of a chemically less specific electronic state with high fluorescence quantum yield, giving it wide applicability as a specific probe of chemical composition and symmetry. This can be especially useful for the analysis of bio-materials since Raman, unlike fluorescence, does not require labeling of the sample. What makes Raman spectroscopy challenging is that its cross section is quite small. Only one in a million photons interacting with a sample will be inelastically scattered and thus exhibit a Raman shift, while the other photons are simply Rayleigh scattered. In order to get enough signal for analysis, acquisition times of several tens of seconds per location may become necessary.

**Raman microscope** — A Raman spectrometer is often combined with an optical microscope to take advantage of the high spatial resolution that a confocal optical setup can offer. The main components of a dispersive Raman setup are a continuous wave laser to illuminate the sample, high NA optics to collect the backscattered radiation, a laser-line rejection filter, and a spectrometer consisting of an entrance slit, a diffraction grating, and a CCD camera.

Analytical spatial resolution is limited by diffraction and for a conventional upright Raman setup is typically 500nm to 1 $\mu$ m with a depth of focus of around 1 $\mu$ m. As an example, the lateral resolution in a transmission mode setup, with an oil-objective NA of 1.2 and red laser light, may be calculated to be 322nm, using the Rayleigh criterion:

$$R = 0.61 \cdot \lambda / NA$$

Bringing AFM and Raman spectroscopy together offers a way to improve this spatial resolution of analysis.

## Combining AFM with Raman Spectroscopy

**Tip Enhanced Raman Scattering (TERS)** — The full synergistic effect of AFM and optical spectroscopies comes into play when the AFM tip is tasked with “becoming the light source.” With the end radius of an AFM tip <20nm, i.e., much smaller than the conventional diffraction limit spot size, 30-50 times higher spatial resolution can be obtained. In near-field microscopy, one uses the effect that a small object brought into a propagative field induces an evanescent wave and vice versa. One of the characteristics of evanescent waves is that they decay exponentially with increasing distance, which offers a gateway to resolution beyond the classical diffraction-based limitations. This requires the light source and sample to be at a distance from each other that is much smaller than the wavelength of light used, i.e., the optical near-field.<sup>6</sup> By using a suitable AFM tip as a scatter light source and subsequently scanning the sample, tip-assisted optical spectroscopy measurements can be performed (see figure 2). A suitable AFM tip is brought into the optical near-field above the sample and illuminated by continuous or pulsed light at wavelengths ranging from the visible to the infrared. The incident radiation is locally enhanced at the tip apex, subsequently interacts with the sample and is scattered back into detectable far-field radiation. A suitable detection scheme analyzes the light in the far-field allowing the measurement of optical signals like

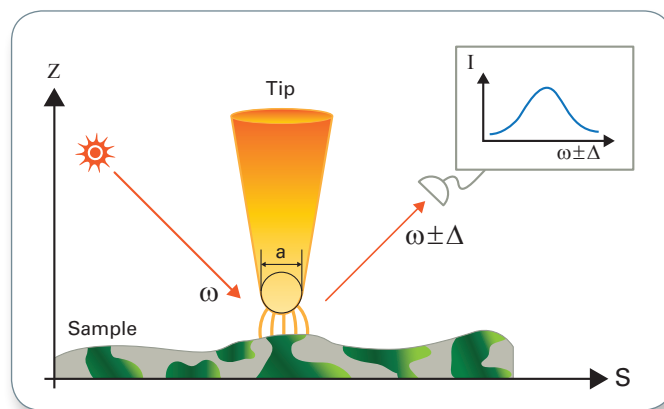


Figure 2. General setup for linear and non-linear tip-assisted Scanning Probe Microscopy (SPM) and optical spectroscopies. A sharp tip is brought into the optical near-field and illuminated from the side. The backscattered light from the tip-sample gap is detected in the far-field using a suitable detection scheme. For TERS the tip has to be metallized so that the surface plasmon can be excited, which will then give rise to the typically seen enhancement factors.

Raman, infrared, or non-linear second-harmonic data with lateral resolution determined by the size of the scattering source, i.e., the AFM tip. These measurements can be accomplished in transmission or reflection geometry, enabling characterization of transparent and opaque samples, respectively.

The Raman signal from the <20nm region defined by an AFM tip normally would be vanishingly small, considering

the inefficiency of the Raman process in addition to the reduction of the collection area from several square-microns for a far-field illumination spot to a submicron-square area for a typical AFM tip. In contrast, the tip apex locally enhances both the incident laser excitation as well as the induced Raman polarization.

The enhancement can be achieved by combining certain metal tips with particular excitation light sources, such as a silver tip with green light and a gold tip with red light. In general coinage metals work well as materials for tip-enhanced Raman scattering (TERS) tips because they exhibit a surface plasmon resonance in the visible range of the spectrum and thus can be excited by the incident laser beam. This strong enhancement is what makes Raman spectroscopy at the nanometer scale feasible.<sup>7</sup> Incidentally, a side illumination scheme as shown in figure 2 has been shown to generate the highest enhancement factor for TERS.<sup>8,9</sup> Because of the strong localization of the electromagnetic field around the tip, TERS exhibits a much higher surface sensitivity than far-field Raman spectroscopy.<sup>10</sup>

In Raman, the polarization of the electromagnetic field along the tip axis has an effect on the selection rules for Raman emission. This can become important when comparing far-field and near-field data.<sup>11</sup> The following experiment demonstrates the importance of polarization control of the incident beam for TERS (see figure 3). An etched gold wire was used as a TERS tip and glued to a tuning fork. The tuning fork was operated at resonance so that the tip was oscillated at an amplitude of about 1nm parallel to the surface. This non-optical feedback method is often referred to as shear-force feedback and keeps the tip in feedback above a Graphene sample without making intermittent contact.<sup>12</sup> Using a waveplate, the incident light polarization was varied from being along the

tip axis (p-polarized) to being perpendicular to the tip axis (s-polarized). The spectrum exhibits the D- and G-band region from 1300 to 1600cm<sup>-1</sup>, and one can see the enhancement effect almost disappeared when s-polarized illumination was used.

Tip-enhanced spectroscopies such as TERS open the door to a whole new field of research. The improvement in spatial resolution is the obvious gain one expects from combining traditional far-field spectroscopies with atomic force microscopy, but there is also a higher sensitivity to surface features. The difference in selection rules between near- and far-field experiments indicates that TERS is similar to conventional Raman spectroscopy but does not just yield the exact same information on a smaller length scale.

### Instrumentation for a Combined AFM-Raman System

The biggest challenge in a combined instrument enabling Raman spectroscopy and nanoscale surface characterization is to avoid compromising the performance of either. Several design factors need to be considered.

**Optical interference** — Typically, Raman measurements are carried out using excitation in the visible regime. To allow parallel, simultaneous operation of the spectrometer and the AFM, the wavelength of the AFM beam-bounce system should be changed to the near-IR so as to not interfere with optical measurements. A better solution is to employ a non-optical feedback system, such as STM or tuning fork feedback.<sup>12</sup>

**Noise** — Spectrometer systems often employ several lasers that may be cooled by noisy external fans or water cooling systems. They also may radiate heat in the proximity of the AFM. Both of these effects can negatively affect AFM performance. Noise from fans can couple into the AFM and cause instabilities in the feedback loop. Temperature changes will cause the AFM to drift and make it extremely difficult to keep the tip in the selected field-of-view.

**Measurement location** — To operate without a compromise in performance, the sample could be shuttled between the AFM and the Raman spectrometer as shown in Figure 4. However, to achieve the benefits of both the AFM's high spatial resolution and TERS, the sample should be scanned underneath the tip, as is done on Bruker's Catalyst and Innova AFMs. This is because the laser beam exciting the plasmon resonance in the AFM tip must be focused onto the tip during the imaging process, thus forcing the AFM imaging to be accomplished by sample scanning. For certain non-TERS co-localized AFM and Raman measurements, i.e., the execution of an AFM and micro-Raman experiment on the sample location, a tip-scanning AFM, such as Bruker's Dimension Icon, can be employed. These co-located measurements do not rely on the near-field enhancement of the AFM tip and are straightforward to perform and interpret as functionalities like ScanAsyst® software automation can be used.<sup>13</sup>

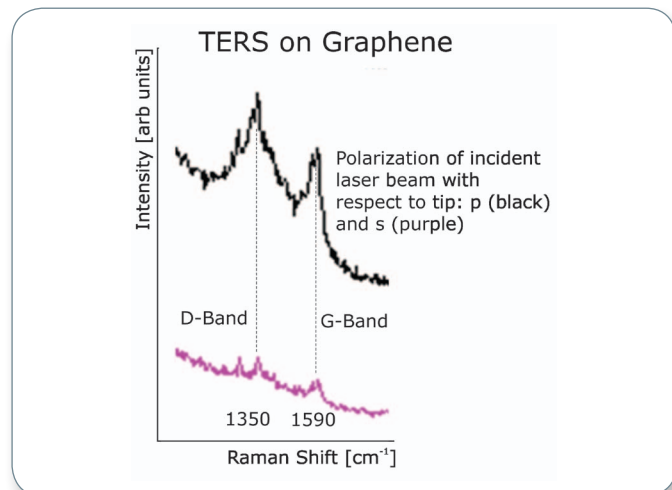


Figure 3. TERS spectra of graphene obtained using a gold tip and tuning fork AFM feedback. It is evident that the TERS effect only happens when the incident light was polarized along the tip axis (p-polarized) and not perpendicular to it (s-polarized). (The authors would like to thank Samuel Berweger/University of Colorado for helping acquire the spectrum.)



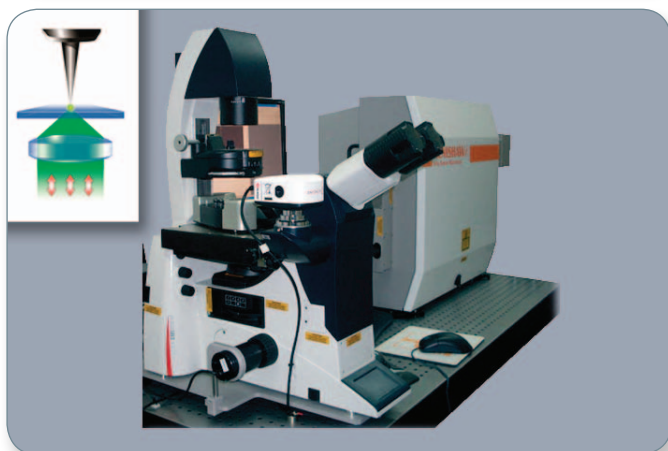
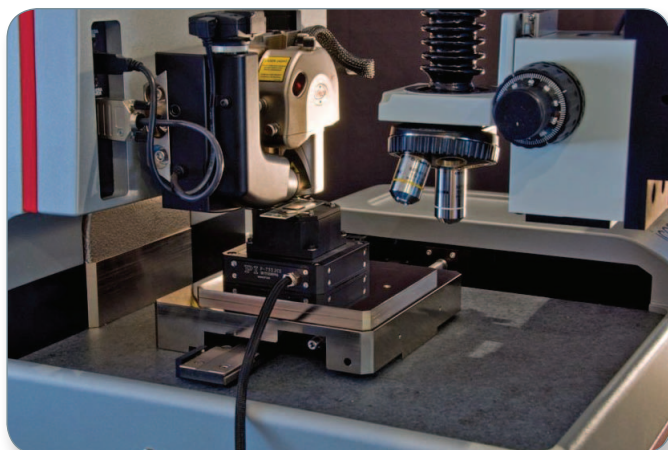


Figure 4. View of the Dimension Icon stage and optics arm of the Raman microscope for co-located AFM-Raman measurements (shown on top). The Icon stage shuttles the sample between the AFM head (left) and the Raman objective (right). The red spot emanating from the objective is the Raman laser illuminating the sample during a Raman measurement. Photos of the sample-scanning Innova-IRIS and Catalyst-IRIS systems for correlated and TERS imaging are shown on bottom.

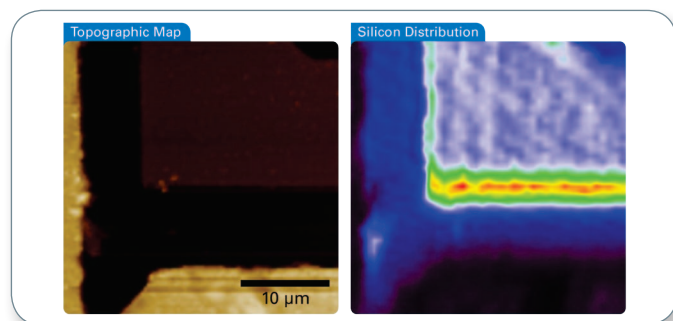


Figure 5. Simultaneous AFM-Raman acquisition sequence with (left) AFM sample topography, and (right) Raman map. The Raman image was created by plotting the intensity of the main silicon band at  $520\text{cm}^{-1}$ . The areas in red, yellow and green depict the areas of exposed silicon. Image size  $30\mu\text{m}$ .

### Co-Localized AFM and Raman Measurements

Co-located, correlated AFM and Raman data acquisition can be accomplished in tip-scanning mode. This mode has many applications even though the spatial resolution of analysis is diffraction-limited for the optical part of the data.

**Semiconductors** — The dataset depicted in figure 5 shows a semiconductor structure with partially buried silicon. The

sample topography acquired by atomic force microscopy shows structures of different physical dimensions on the specimen but lacks chemical information. Chemical information is available in the Raman map on the right that is based on integration of the silicon peak at  $520\text{cm}^{-1}$ . The areas in red, yellow, and green are exposed silicon.

**Graphene** — Atomic force microscopy and Raman are often used to study the material properties of graphene and carbon nanotubes.<sup>5</sup> Here we show that the combination of quantitative nanomechanical measurements (QNM) and Raman spectroscopy can enable a better understanding of these materials. The intensity of the graphene G-band around  $1580\text{cm}^{-1}$  and the shape of the 2D-band around  $2700\text{cm}^{-1}$  can be used as a measure of the number of layers. The intensity of the D-band around  $1350\text{cm}^{-1}$  indicates disorder of the lattice. Figure 6 shows AFM and Raman images of the G and D-band of a graphene flake prepared on silicon oxide. Correlations of the data unambiguously reveal the layered structure and the 300pm step height between subsequent layers. The D-band image also hints at an area of increased defects along the edge of the single portion of the sample. This area was subsequently investigated using the QNM capabilities

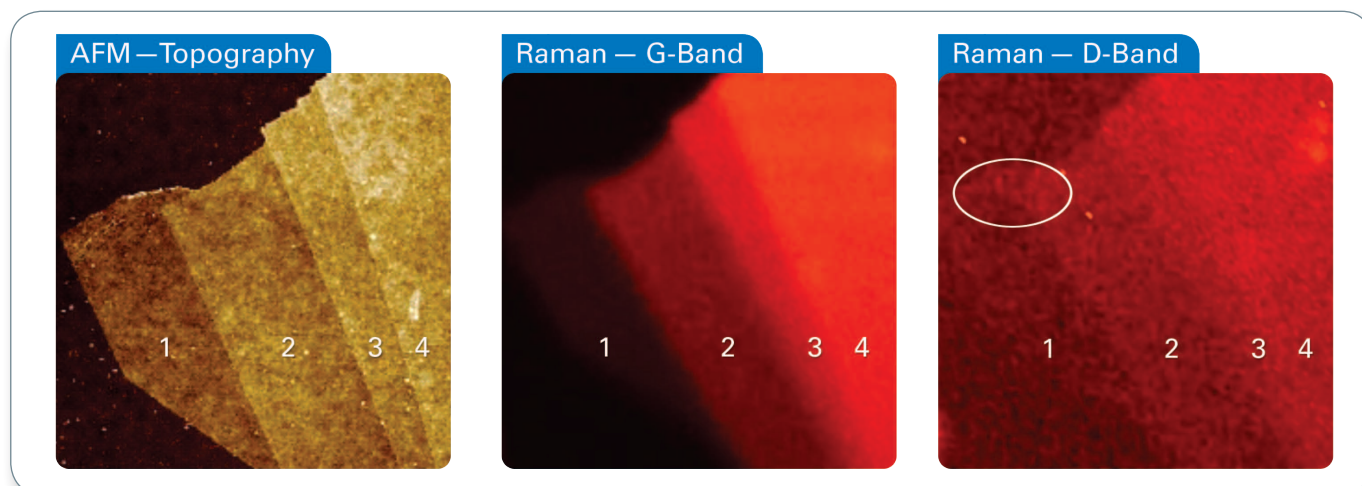


Figure 6. AFM topography (left) and Raman images of the G (middle) and D-band (right) of a graphene flake on silicon. Both Raman and AFM data confirm the layered structure with 300pm step height separating layers. The Raman image of the D-band also suggests an increased density of defects along the edge of the single layer (see circle). Image width is 15µm.

of the AFM. Figure 7 shows four channels (topography, adhesion, modulus, and deformation) of QNM data from a 2.5µm scan size. In the topographic map we can identify some wrinkle like structures. These structures exhibit softer compliance and reduced adhesion compared to the undisturbed portion of the layer). The deformation channel additionally shows a larger deformation on the graphene flake when compared to the substrate and lets us deduce that the graphene flake does not mechanically relax during the sub-millisecond contact time of the QNM measurement. Thus, the combination of co-located AFM

and Raman data has allowed us not only to easily find and identify relevant features on the sample but also to further investigate their mechanical behavior in detail.

### TERS Measurements

Higher spatial resolution of analysis is possible with TERS, and molecular studies are a major interest.<sup>14</sup> The following dataset depicts experiments on malachite green, a molecular system that has been used in the literature to demonstrate single molecule sensitivity of TERS.<sup>15</sup> Figure 8 shows sets of Raman spectra taken at different heights of the tip above the sample. With the tip in feedback, the spectrum, shown in red, nicely displays the characteristic bands that let one identify the functional groups of malachite green. With the sample just pulled away 60nm, but the laser spot still focused onto the tip, it is evident that the TERS effect vanished and the spectrum, shown in black, is now purely generated by the far-field interaction. Both spectra were taken using the same integration time of 1 second. The ratio in intensity between the peak intensity in the near-field and far-field normalized to the different illumination areas is the TERS enhancement factor, and typically ranges from  $10^4$  to  $10^8$  depending on the combination of tip-sample used in a specific experiment. These so called tip checks are highly recommended in TERS to avoid the danger of getting a spectrum from material that the tip accidentally picked up.<sup>16</sup>

Another often overlooked fact is that multiple scattering events between the metallic tip and the sample can give rise to a signal enhancement that is not caused by a near-field effect.<sup>17</sup> Besides careful polarization control, tip-sample approach curves, and good confocality of the Raman system employed, checking that the TERS signal changes reproducibly at distances well below the diffraction limit is another important step. This is shown in figure 9. After a topographic scan was taken, the tip was parked at the location indicated by the blue/red dot shown in the topographic data and a TERS spectrum was acquired. Under

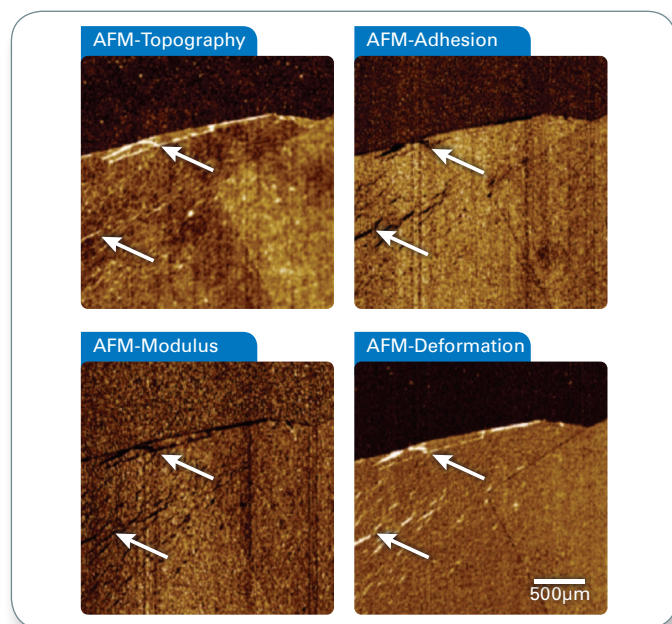


Figure 7. Simultaneously recorded quantitative nanomechanical AFM data of a single and double layer of the graphene flake. The wrinkles marked by arrows visible in the topography (top left) are strongly reflected in the mechanical property channels as being softer (bottom left) with less adhesion (top right) than the surrounding material. The deformation channel (bottom right) points to a strong plastic deformation of the Graphene layers as they do not relax during the sub-millisecond contact time with the AFM probe. Image size 2.5µm.



### TERS on Malachite Green

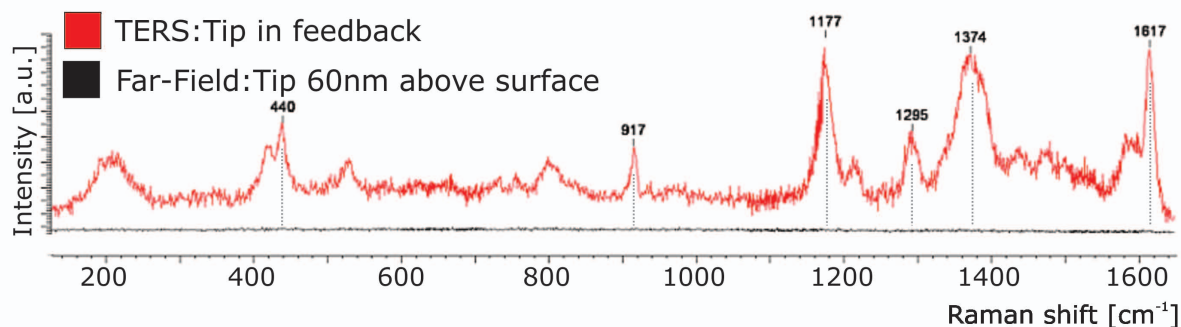


Figure 8. Tip-assisted Raman spectroscopy spectra of malachite green obtained using a gold tip illuminated by 633nm light at varying distances above the surface. The red spectra was obtained with the tip in feedback whereas the black spectrum was collected with the sample pulled 60nm away from the tip. By comparing the peak intensities with the tip approached to the retracted spectra, one can clearly see the striking enhancement of Raman modes.

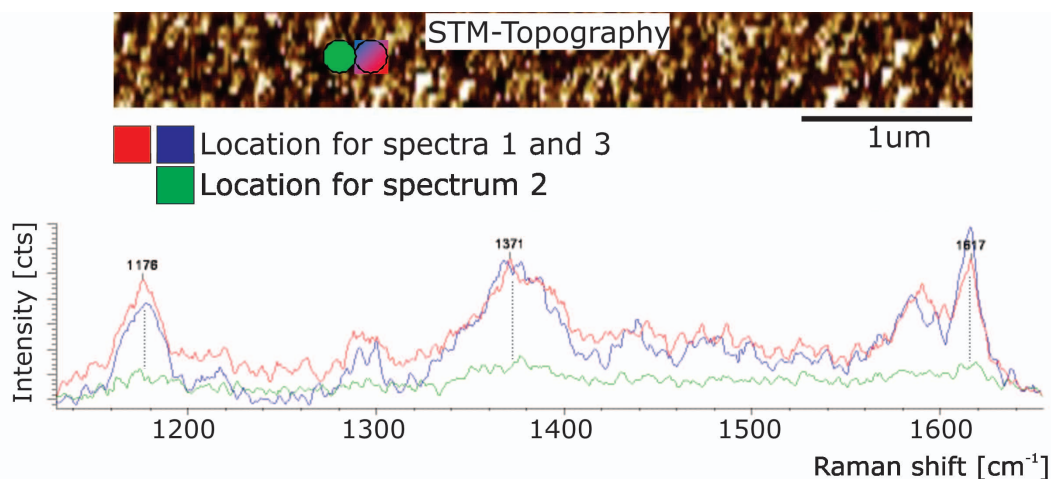


Figure 9. TERS spectrum of malachite green obtained using the Innova IRIS at two different locations separated by <90nm indicated by the blue and green dots in the above SPM image. The first spectrum at location 1 is displayed in blue, the second second spectrum at location 2 in green, and the third second spectrum back at location 1 is shown in red proving the sub-diffraction lateral resolution capabilities and reproducibility.

closed-loop control the tip was then moved to the location marked by the green dot and another Raman spectrum was taken. To verify that no sample damage occurred the tip was moved back to the original starting position and another spectrum was recorded. The intensity changes in the spectra between the two locations demonstrate that the resolution is indeed sub-wavelength and that no sample or tip damage occurred during the data acquisition. Lateral resolution for TERS is related to the active area of the signal enhancing tip and typically somewhere in the range of 10nm to 20nm.

Stress in materials can have a severe impact on device functionality and hence is an important parameter to know and control. Raman scattering is a good methodology for measuring stress in silicon devices by analyzing the shift of the first order Raman band at 520  $\text{cm}^{-1}$ . Unfortunately, the diffraction limit restricts those measurements to typically 1 $\mu\text{m}$  lateral resolution. Using TERS, one can extend

those measurements to resolutions in the order of a few nanometers. Figure 10 shows a spectral measurement obtained on a model device consisting of a 70nm layer of strained silicon residing on top of an ultrathin barrier layer of BaOx followed by bulk Si. As the TERS tip approaches the sample, the increased signal from the strained Si-layer is readily apparent. This opens the door for further studies and a variety of applications on silicon devices.

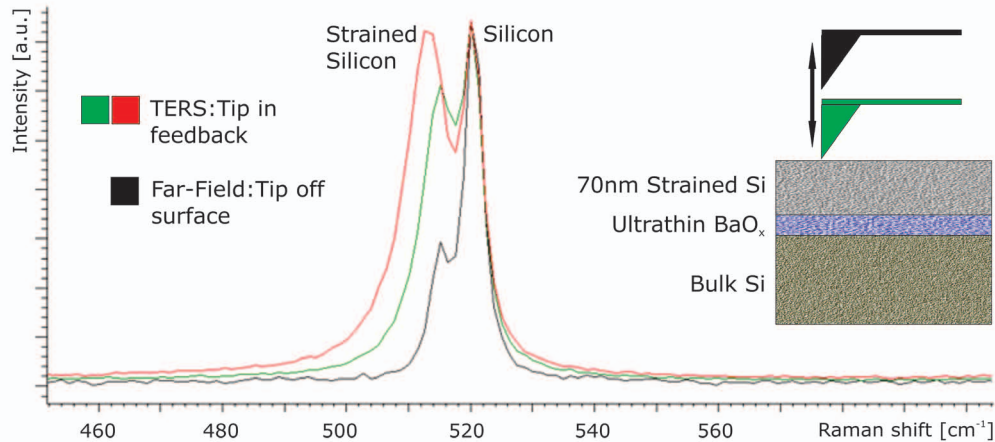


Figure 10. Tip enhanced Raman spectrum of Si device with 70nm thick strained Si layer on ultrathin BaO<sub>x</sub> followed by bulk Si. The increased signal from the strained Si layer upon tip approach is readily apparent. Courtesy of D. Kosemura, Meiji University, Japan.

## Conclusion

Co-localized AFM and Raman instrumentation allows researchers to interrogate samples using both scanning probe techniques and optical spectroscopy, yielding detailed information about nanoscale properties and composition. Diffraction-limited AFM-Raman experiments are straightforward as is the interpretation of data. TERS provides chemical information on the nanometer scale. TERS experiments are straightforward to execute but may require special consideration of the tip-sample interaction in the optical near-field for data interpretation.

## References

1. G. Binnig, C. Quate, and Ch. Gerber, "Atomic Force Microscope," *Physical Review Letters* 56 (1986): 930-33.
2. H. Kuzmany, *Solid State Spectroscopy*, 2nd edition, Springer: Heidelberg, 2009.
3. D. Harris and M. Bertolucci, *Symmetry and Spectroscopy*, Oxford University Press: New York, 1989.
4. S. Berweger, C. Neacsu, Y. Mao, H. Zhou, S. Wong, and M. Raschke, "Optical nanocrystallography with tip-enhanced phonon Raman spectroscopy," *Nature Nanotechnology* 4 (2009): 469-99.
5. R. Saito, M. Hoffmann, G. Dresselhaus, A. Jorio, and M.S. Dresselhaus, "Raman spectroscopy of graphene and carbon nanotubes," *Advances in Physics* 60, 3 (2011): 413-550.
6. E.H. Synge, "A suggested method for extending the microscopic resolution into the ultramicroscopic region," *Philosophical Magazine* 6 (1928): 356-62.
7. A. Hartschuh, "Tip-Enhanced Near-Field Optical Microscopy," *Angewandte Chemie* 47 (2008): 8178-91.
8. A. Downes, D. Salter, and A. Elfick, "Finite Element Simulations of Tip-Enhanced Raman and Fluorescence Spectroscopy," *Journal of Physical Chemistry B* 110 (2006): 6692-98.
9. Z. Yang, J. Aizpurua, and H. Xu, "Electromagnetic field-enhancement in TERS configurations," *Journal of Raman Spectroscopy* 40 (2009): 1343-48.
10. R. Stöckle, Y. Suh, V. Deckert, and R. Zenobi, "Nanoscale chemical analysis by tip-enhanced Raman spectroscopy," *Chemical Physics Letters* 318 (2000): 131-36.
11. T. Ichimura, S. Fujii, P. Verma, T. Yano, Y. Inouye, and S. Kawata, "Subnanometric Near-Field Raman Investigation in the Vicinity of a Metallic Nanostructure," *Physical Review Letters* 102 (2009): 186101.
12. W.H.J. Rensen, Ph.D. thesis, University of Twente (2002).
13. S.B. Kaemmer, Bruker Applications Note 133 (2011).
14. J. Steidtner and B. Pettinger, "Tip-enhanced Raman spectroscopy and microscopy on single dye molecules with 15 nm resolution," *Physical Review Letters* 100 (2008): 236101.
15. C.C. Neascu, J. Dreyer, N. Behr, and M.B. Raschke, "Scanning probe Raman spectroscopy with single molecule sensitivity," *Physical Review B* 73 (2006): 193403.
16. K. Domke and B. Pettinger, "Studying Surface Chemistry beyond the Diffraction Limit: 10 Years of TERS," *ChemPhysChem* 11 (2010): 1365-73.
17. R. Ramos and M. Gordon, "Near-field artifacts in tip-enhanced Raman spectroscopy," *Applied Physics Letters* 100 (2012): 213111.
18. I. De Wolf, "Micro-Raman spectroscopy to study local mechanical stress in silicon integrated circuits," *Semiconductor Science and Technology* 11 (1996): 139-54.

## Author

Stefan Kaemmer, Ph.D., Bruker Nano Surfaces  
(stefan.kaemmer@bruker-nano.com)

## Acknowledgements

The author would like to thank Markus Raschke, Samuel Berweger, and Joanna Atkin (University of Colorado/Boulder) for many fruitful discussions and help during TERS measurements. The help of D. Kosemura (Meiji University/Japan) for designing the silicon device and assistance with data acquisition is greatly appreciated. Finally, the guidance of Tim Batten and Tim Prusnik (Renishaw) for analyzing Raman data is highly valued.

## ● Bruker Nano Surfaces Division

Santa Barbara, CA · USA  
+1.805.967.1400/800.873.9750  
productinfo@bruker-nano.com

[www.bruker.com](http://www.bruker.com)